Science of the Total Environment 648 (2019) 1500–1510

Contents lists available at ScienceDirect

Science of the Total Environment

journal homepage: www.elsevier.com/locate/scitotenv

Long-term agricultural management and erosion change soil organic matter chemistry and association with minerals

Xiang Wang, Nicolas A. Jelinski, Brandy Toner, Kyungsoo Yoo *

Department of Soil, Water, and Climate, University of Minnesota–Twin Cities, Saint Paul, MN 55108, USA

HIGHLIGHTS

- Cultivation reduced $SSA_{SOM\text{-}covered}$ regardless of landscape position.
- Depositional soils had a higher proportion of $SSA_{SOM\text{-}covered}$ than eroding soils.
- SSA contributed by Fe oxyhydroxides were lower in cultivated than grassland topsoil.
- Phenolic and aliphatic C peaks were weaker in cultivated eroding soils.

GRAPHICAL ABSTRACT

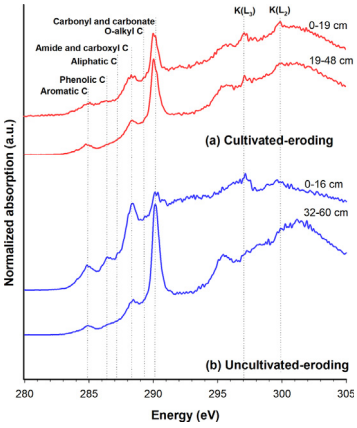

ARTICLE INFO

Article history:
Received 31 May 2018
Received in revised form 4 August 2018
Accepted 8 August 2018
Available online 9 August 2018

Editor: Jay Gan

Keywords:
Cultivation
Erosion
Mineral-associated soil organic matter
Specific mineral surface area
XANES

ABSTRACT

The interaction of soil organic matter (SOM) and minerals is a critical mechanism for retaining SOM in soil and protecting soil fertility and long-term agricultural sustainability. The chemical speciation of carbon (C) and nitrogen (N) in mineral-associated SOM can be sensitive to both anthropogenic management practices and landscape positions, but these two aspects are rarely examined in tandem. Here we examined the effects of long-term (>100 years) agricultural management and erosion on mineral-associated SOM along grassland and agricultural hillslope transect. The mineral-associated SOM was obtained using particle size and density fractionation approaches. Chemical speciation of C and N in mineral-associated SOM was characterized using micro X-ray absorption near-edge fine structure (XANES) spectroscopy. The extent of SOM coverage and contribution of iron oxyhydroxides (Fe oxides) to the total specific mineral surface area (SSA) were determined using the BET–N_2 adsorption method of soil samples under three conditions: untreated, SOM removal, and Fe oxides removal. The amount of SSA covered by SOM ($SSA_{SOM\text{-}covered}$) was lower by 61% and 37% in cultivated eroding and depositional topsoils, respectively, compared with the corresponding grassland. Depositional soils had higher $SSA_{SOM\text{-}covered}$ than eroding positions. In the cultivated hillslopes, aromatic and phenolic C species were more abundant in depositional soils than in the eroding topsoils, indicating that deposition and burial of eroded or in-situ plant-derived phenolic C protected them from further transformation. Our results, therefore, highlight the importance of anthropogenic activities in the interaction of SOM and minerals, including C speciation changes, which may exert a considerable influence on SOM retention in soils.

* Corresponding author.
E-mail address: kyoo@umn.edu (K. Yoo).

https://doi.org/10.1016/j.scitotenv.2018.08.110
0048-9697/

1. Introduction

Mineral-associated soil organic matter (SOM) comprises a significant proportion of the total SOM (Jackson et al., 2017; Kleber et al., 2015; Kögel-Knabner et al., 2008) and plays a critical role in sustaining soil quality and sustainable agricultural productivity (Amundson et al., 2015). Cultivation and subsequent erosion are two of the primary factors driving SOM losses in human-managed landscapes (Martens et al., 2004; Papiernik et al., 2009a, 2009b; Solomon et al., 2007; Zhu et al., 2014). Numerous studies have documented that cultivation-induced losses or gains of SOM are often dependent on topographic position (Don et al., 2011; Van Oost et al., 2012; Prokop et al., 2018; Zhu et al., 2014). Recent estimates show that agricultural land use may have resulted in the loss of 133 Pg C for the top 2 m of soil and that the loss rates have increased dramatically in the past 200 years (Sanderman et al., 2017). Losses of SOM associated with agricultural activities under conditions of erosion or soil loss typical of upper hillslope positions have been commonly attributed to enhanced microbial decomposition and the physical removal of soil particles through erosive processes (Amundson et al., 2015; Besnard et al., 1996; Don et al., 2011). However, at lower hillslope positions experiencing burial and deposition, cultivation may increase SOM stocks (Doetterl et al., 2012; Papiernik et al., 2007). Consequently, whether net effects of cultivation and erosion could act as an atmospheric carbon source or sink is a hotly debated topic (Lal, 2003; Van Oost et al., 2007).

Among the pools of SOM affected by agriculture and erosion, mineral-associated SOM is particularly important because it is the portion of SOM most closely associated with fine particles (clay and fine silt) and iron oxyhydroxides (Fe oxides hereafter) (Eusterhues et al., 2005; Kaiser and Guggenberger, 2003; Kögel-Knabner et al., 2008; Mikutta and Kaiser, 2011). Iron oxides can represent a substantial fraction of secondary minerals in soils and may have even higher affinities for SOM than the phyllosilicates (Eusterhues et al., 2005; Mikutta et al., 2006; Pronk et al., 2011; Wagai et al., 2009). Because Fe oxide minerals provide reactive surfaces as binding sites for SOM (Kögel-Knabner et al., 2008; Pronk et al., 2011), Fe oxide surface area ($SSA_{Feoxide}$) should contribute to the amount of SSA covered by SOM ($SSA_{SOM\text{-}covered}$), as well as the overall retention of SOM (Eusterhues et al., 2005; Lyttle et al., 2015; Mayer and Xing, 2001; Pronk et al., 2011; Wagai et al., 2009).

The chemical speciation of C and N in mineral-associated SOM may also play an important role in understanding the retention of organic matter in soils (Chen and Sparks, 2015; Kleber et al., 2015). This is relevant to assessing agricultural impacts on SOM because long-term cultivation has the potential to decrease total SOM storage, stabilization, and turnover time (Dignac et al., 2017; Papiernik et al., 2007; Pisani et al., 2016) but may also change the chemistry of SOM associated with minerals (Cusack et al., 2013; Ellerbrock et al., 2016; Helfrich et al., 2006; Solomon et al., 2007). Although the interactive effects of soil cultivation and erosion on the quantity of mineral-associated SOM have been investigated extensively (Berhe et al., 2012; Ellerbrock et al., 2016; Guggenberger et al., 1995; Solomon et al., 2007; Wang et al., 2014), few studies have examined the effects of both SOM properties (C and N speciation) and minerals' surface characteristics (percent $SSA_{Feoxide}$) (Chen and Sparks, 2015; Mikutta et al., 2007).

The objectives of this comparative study were to examine the effects of long-term (>100 years) agricultural management and erosion on (i) the relative sizes and sources of mineral-associated SOM, (ii) the chemical speciation of C and N in mineral-associated SOM, and (iii) the mineral surface area covered by SOM as a function of topographic positions in an agricultural hillslope relative to an adjacent hillslope under natural vegetation. By achieving these objectives, we attempt to examine how the critical interactions between SOM and mineral surfaces are affected simultaneously by agriculture and erosion.

2. Materials and methods

2.1. Site description

Our study area lies approximately 3 km north of the town of Cyrus, Minnesota, U.S.A. (−95.74 W, 45.67 N), and consists of paired sampling sites along an uncultivated, grassed hillslope and a cultivated field of ~2.7 ha De Alba et al., 2004; Jelinski, 2014; Li et al., 2008; Papiernik et al., 2005, 2007), approximately 800 m apart, separated by the Chippewa River (Fig. 1). Of the total of eight sampling locations chosen for this study, two sampling locations were selected to represent upper (eroding) and lower topographic positions (depositional) on each of two hillslopes within the cultivated (~40 m) and uncultivated sites (~70 m), respectively (Fig. 1). At each of these sampling locations, soil samples representing morphologically distinct genetic horizons were obtained, thus sample depth increments represent horizon thicknesses and not pre-defined depth increments (Table 1).

Rates of soil erosion and deposition estimated from foundational research in the vicinity of the study area suggest that rates of erosion and deposition processes are approximately 2 orders of magnitude greater on the cultivated site than the uncultivated site (Jelinski, 2014; Li et al., 2007; Papiernik et al., 2007). Soil loss estimates derived from process-based models (WATEM, WEPP, TillEM) and ^{137}Cs-based radioisotope conversion models for water erosion at the cultivated erosional sites range from 20 to >50 Mg ha yr^{-1}, while estimated soil deposition rates at the depositional points on the cultivated site range from 10 to >30 Mg ha yr^{-1} (Jelinski, 2014; Li et al., 2007; Papiernik et al., 2007). Long-term soil loss estimates derived from ^{10}Be conversion models at the eroding positions of the uncultivated site range from 1 to 2 Mg ha^{-1} yr^{-1}, while long-term deposition estimates at the uncultivated site are approximately 0.8 Mg ha^{-1} yr^{-1} (Jelinski, 2014). Therefore, we refer to upper hillslope positions as eroding positions and the lower hillslope positions as depositional positions for both the cultivated and uncultivated sites throughout the remainder of the text.

Surficial sediments in the study area are comprised of Wisconsin-age calcareous glacial till on the uplands, with Holocene alluvial sediments in river valleys (Harris, 2003). Upland soils in the study area are dominated by Mollisols and Inceptisols (Soil Survey Staff, 2014; Chernozems and Cambisols in the WRB system (IUSS Working Group WRB, 2014). Documentary evidence of lack of extensive cultivation on the uncultivated hillslope includes the earliest archived aerial photos taken in 1939 CE (UMN, 2017). Additionally, the uncultivated hillslope transect is recognized as a dry prairie native plant community of statewide importance (MCBS, 2003), which suggests that post-European settlement land use intensity on this hillslope has been minimal.

The cultivated field had been under agricultural management for >100 years and under a conventional tillage management regime (annual moldboard plow and secondary tillage) for at least 40 years prior to sampling. A central pivot irrigation system was installed on the cultivated field in 2007. On the cultivated site, the dominant cropping system is a rotation of corn (*Zea mays*), soybean (*Glycine* max), and wheat (*Triticum aestivum*). Anhydrous ammonia (130 kg of N ha^{-1}) and granular fertilizer (240 kg ha^{-1} of 27-70-40) were applied in the cultivated field (Papiernik et al., 2009a, 2009b).

2.2. Soil physical and chemical characterization

Soil pH was determined in a 1:1 slurry of 10 g of air-dried soil and 10 mL of 0.01 M $CaCl_2$. Total carbon and nitrogen (g kg^{-1}) were determined by dry combustion at 800 °C using a LECO 2000 CN analyzer (LECO Corporation). Organic carbon (OC) concentrations (g kg^{-1}) were determined by subtracting inorganic carbon concentrations (determined by modified pressure calcimetry) from total carbon concentrations.

Samples for particle size analysis were air-dried, passed through a 2-mm sieve, and hand homogenized prior to subsampling. Three 0.5 g

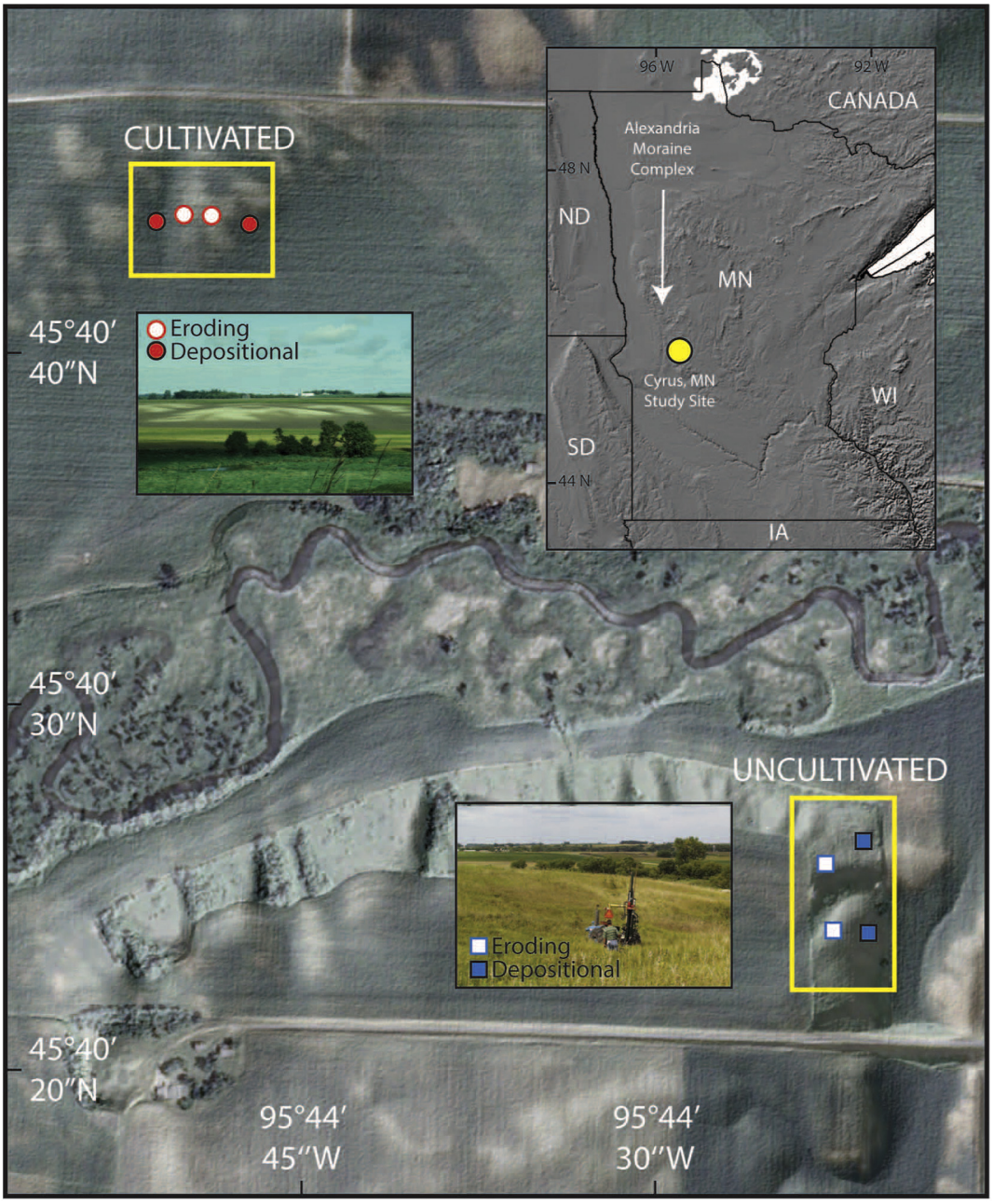

Fig. 1. Topographic locations of the cultivated and uncultivated hillslope transects. Inset photos courtesy of S.K. Papiernik (upper) and T.E. Schumacher (lower).

subsamples were then obtained and dispersed overnight in Na-hexametaphosphate prior to standard analysis on a Malvern Mastersizer 3000. We assumed the refractive indices of our soil and the water-based dispersant to be 1.549 and 1.33, respectively (Miller and Schaetzl, 2012). We ran extensive in-house validation on known size fractions of sand, silt, and clay to optimize our laser particle size

Table 1
Selective soil properties from the eroding and depositional area in the cultivated and uncultivated grassland soils (data from Jelinski, (2014)). ND represented Not Determined.

Sites	Slope	Curvature	Horizon	Depth	pH ($CaCl_2$)	SOC (%)	Inorganic C (%)	TN (%)	C/N ratios	Sand (%)	Silt (%)	Clay (%)
Cultivated eroding	0.07	0.04	Ap	0–19	7.52	0.97	2.54	0.09	10.35	34	41	25
Cultivated eroding			Bk	19–48	ND	0.30	2.67	0.03	11.44	41	43	16
Cultivated depositional	0.08	−0.01	Ap	0–22	7.31	1.44	0.55	0.12	12.43	38	40	22
Cultivated depositional			AB	22–55	7.07	1.17	0.10	0.09	12.85	45	35	20
Cultivated depositional			Bw1	55–82	7.05	0.53	0.00	0.03	17.26	48	25	27
Uncultivated eroding	0.22	0.05	A	0–16	7.29	3.86	0.31	0.32	12.03	36	37	27
Uncultivated eroding			Bk1	32–60	7.47	1.02	3.39	0.07	14.25	41	35	24
Uncultivated depositional	0.15	−0.02	A	0–23	5.73	4.04	0.01	0.28	14.54	33	49	18
Uncultivated depositional			AB	23–47	5.52.	1.18	0.00	0.15	8.05	37	43	20
Uncultivated depositional			Bw1	47–67	5.83	0.37	0.55	0.08	4.49	42	45	13

data for comparison with the more traditional hydrometer method. Based on this in-house compilation, we set the clay-silt break to be 8 μm, which is consistent with other studies (Konert and Vandenberghe, 1997). To eliminate bias due to small subsample sizes, we ran triplicate analyses of each of our three subsamples and compared the data statistically. We then discarded the set of three that was most different from the other (two) subsamples. The two most comparable triplicate sets were then used to calculate the mean particle size distribution ($N = 6$) for use in subsequent analyses.

2.3. Specific mineral surface area (SSA)

In measuring specific mineral surface area (SSA), we combined Brunauer-Emmett-Teller (BET) theory (Brunauer et al., 1938) with a TriStar 3020 Surface Area and Porosity Analyzer in the Department of Soil, Water, and Climate at the University of Minnesota. The BET-N_2 method does not capture interlayer surface areas of expandable clays (Heister, 2014; Wagai et al., 2009), and therefore our SSA determined by the BET-N_2 method should be considered to represent the external surface of solids present in soil samples. To quantify total SSA (SSA_{total}), soil samples were treated by heating at 350° C for 12 h to remove SOM (Lyttle et al., 2015; Mayer and Xing, 2001; Wagai et al., 2009; Wang et al., 2018). The difference between total SSA and SSA measured on the soil samples prior to heating was considered as SSA covered by SOM ($SSA_{SOM\text{-}covered}$). The percentage of SSA covered by SOM was then calculated using eq. 1. To measure mineral surface area contributed by Fe oxides ($SSA_{Feoxide}$), SSA was measured following the heating (350 °C for 12 h) and removal of Fe oxides with a dithionite-citrate extraction (Eusterhues et al., 2005; Pronk et al., 2011; Wissing et al., 2014). The percentage of SSA contributed by Fe oxides ($SSA_{Feoxide}$) was calculated using Eq. (2).

$$SSA_{SOM-covered}(\%) = \frac{SSA_{total} - SSA_{before}}{SSA_{total}} \times 100 \quad (1)$$

$$SSA_{Feoxide}(\%) = \frac{SSA_{total} - SSA_{oxides\ removal}}{SSA_{total}} \times 100 \quad (2)$$

As a proxy for SOM loading on mineral surfaces, soil organic C (SOC; mg g^{-1} soil) to the total specific mineral surface area (m^2 g^{-1} soil), i.e. SOC/SSA_{total} ratio (mg m^{-2}), is calculated as an operational measure to normalize organic carbon relative to mineral surface area (Fisher et al., 2018; Wagai et al., 2009; Wang et al., 2018).

2.4. Citrate-dithionite extractable iron (Fe) oxide content

The extractable Fe oxide content of the bulk soils ($N = 41$) was determined by using the dithionite-citrate-bicarbonate method (Mehra and Jackson, 2013; Soil Survey Laboratory Methods Manual, 2014). Briefly, up to 5 g soil were exacted by 0.3 M sodium citrate-bicarbonate solution and 1 g sodium dithionite. Then samples were shaken overnight (15 h) before centrifuge. This operational fraction is often assumed to represent the total pedogenic Fe oxide content of most soils (Soil Survey Laboratory Methods Manual, 2014). Concentrations of the dithionite-extractable Fe were determined by inductively coupled plasma optical emission spectroscopy on a Perkin Elmer Optica 3000 ICP Spectrometer with simultaneous CCD detectors at the University of Minnesota Research Analytical Laboratory (http://ral.cfans.umn.edu/).

2.5. Isolation of the mineral-associated SOM

In this study, we used a particle size and density fractionation approach to isolate the fine heavy fraction (<250 μm and >2.0 g cm^{-3}) in which SOM is physically or chemically associated with minerals (Lyttle et al., 2015; Sollins et al., 2009; Wang et al., 2018). Briefly, approximately 10–20 g of air-dried soil samples were passed through a 250 μm sieve to selectively remove fine roots and coarse sand materials. The remaining <250 μm fractions were then mixed with 2.0 g cm^{-3} sodium polytungstate (NaPT) and placed on a shaker for 2.5 h at room temperature. This procedure separates organic debris (<2 g cm^{-3}), in which SOM is defined as the "fine particulate" SOM, and the remainder of SOM is associated with minerals. Minerals dense enough to settle (>2 g cm^{-3}) were retrieved and rinsed with deionized water until the electrical conductivity of the solution was <50 μS cm^{-1}. All samples were oven-dried at 60 °C and weighed to obtain the mass proportion of each fraction relative to the bulk soil.

2.6. Carbon and nitrogen XANES analysis

Carbon and N 1 s X-ray absorption near edge structure (XANES) spectra were collected for the fine heavy soil fractions (<250 μm and >2.0 g cm^{-3}: $N = 10$) using the microprobe version of the Spherical Grating Monochromator (SGM) beamline 11ID-1 at the Canadian Light Source (CLS, Saskatoon, SK, Canada) (Regier et al., 2007). Sample preparation and measurement procedures were based on those developed by Gillespie and co-workers that seek to minimize the radiation dose received by the sample and eliminate spectral artifacts that can arise from substrate effects and normalization (Gillespie et al., 2015). Briefly, subsamples of fine heavy fractions were suspended in deionized water, applied as droplets to freshly prepared Au-coated Si wafers, and dried at room temperature. Carbon and N XANES spectra were recorded in partial fluorescence yield by a single Silicon Drift Detector. The photon energy was scanned continuously across the absorption edge (270 to 320 eV for C; 370 to 440 eV for N) in 30 s. Multiple measurements are taken on fresh, unexposed portions of each sample and then averaged to produce spectra that have sufficient signal to noise ratio and are representative of the sample.

An I-zero spectrum was collected in partial fluorescence yield mode with a Silicon Drift Detector positioned at 90 degrees with respect to the incident beam (Regier et al., 2007). This geometry was selected to maximize the contribution of elastic scattering. The spectral characteristics of the I-zero spectrum were monitored at approximately 12 he Kirkpatrick-Baez mirrors were cleaned on approximately 36 h intervals to eliminate C contamination.

For the monochromator calibration, the characteristic strong absorption peak at 290.1 eV for the mineral calcite was used (Brandes et al., 2004). The 1 s → π* vibrational manifold of N_2 gas evolved from $(NH_4)_2SO_4$ at 400.8 eV was used to calibrate the monochromator for N (Gillespie et al., 2008). Data were averaged in the program *Nexpy* (http://sgm.lightsource.ca/) using beamline-specific macros. Spectra were subjected to energy calibration, pre-edge subtraction, and post-edge normalization in the program Athena (Ravel and Newville, 2005). Carbon features were assigned based on a review of the literature as: (1) aromatic at 284.8 eV; (2) phenolic at 286.4 eV; (3) aliphatic at 287.2 eV; (4) amide and carboxyl C at 288.4 eV; (5) *O*-alkyl at 289.3 eV;, and (6) carbonyl and carbonate at 290.1 eV (Gillespie et al., 2011; Kleber et al., 2011; Solomon et al., 2005). Nitrogen features were assigned based on a review of the literature as: (1) aromatic-N in 6-membered rings at 398.8 eV (heterocyclic-N); (2) nitrilic and aromatic N in 5-membered rings at 399.9 eV (pyrazolic); (3) amide with possible contributions from pyrroles at 401.3 eV (amide); (4) alkyl-N, inorganic NH_4^+; and the 1 s → σ* feature at 406.0 eV (alkyl-N) (Gillespie et al., 2008; Jokic et al., 2004; Leinweber et al., 2007).

2.7. Data analysis

In the surface soil, the values of SSA_{total}, $SSA_{SOM\text{-}covered}$, $\%SSA_{SOM\text{-}covered}$, $SSA_{Feoxide}$, and $\%SSA_{Feoxide}$ were averaged from the eroding and depositional positions of two cultivated and uncultivated landforms, respectively. One-way ANOVA was used to evaluate differences between eroding and depositional in cultivated and uncultivated

hillslopes, respectively, with the Sigmaplot software version 13.0. In this study, we considered differences as statistically significant at $P < 0.05$.

3. Results

3.1. Specific mineral surface area (SSA) of bulk soil covered by organic matter

Little difference in SSA_{total} was found between the eroding and depositional soils at both cultivated and uncultivated sites (Fig. 2a and b). In contrast, $SSA_{SOM\text{-}covered}$ (Fig. 2c and d) and its contribution to SSA_{total} (Fig. 2e and f) were higher in depositional soils than in eroding soils regardless of land use, however. This difference was particularly pronounced on the cultivated hillslope. Regardless of topographic position, cultivated soils had a lower % $SSA_{SOM\text{-}covered}$ relative to the uncultivated grassland. For eroding topsoils, SOM covered 49% and 88% of SSA_{total} in the cultivated field and uncultivated grassland, respectively. The depositional topsoil in the cultivated site had 72% of the mineral surface area covered by SOM, which is relatively smaller than the 88% observed for the uncultivated grassland depositional sites. The size and percentage of SSA covered by SOM generally decreased with increasing depth at all sites, but at both slopes, such depth-dependent patterns were less prominent in the depositional soils.

3.2. Soil organic carbon loading to minerals (SOC/SSA_{total})

The amount of soil organic carbon in the fine heavy fraction can be used as a proxy for mineral-associated SOM. SOC loading to minerals ranged from 0.14 to 2.70 mg OC m^{-2} and decreased sharply with increasing depth for all soil pits (Fig. 3). In the top 40 cm, the SOC loading to minerals was >1 mg OC m^{-2} in the uncultivated soils. Between comparable soil depths, the cultivated soil had relatively lower SOC loading compared with the uncultivated soil regardless of topographic positions. For comparable depths, depositional positions had higher SOC loading than eroding positions across cultivated and uncultivated hillslopes. For example, in the topsoil, the average SOC loading was 0.67 and 1.18 mg OC m^{-2} in the eroding and depositional sites in the cultivated hillslopes while the values were 1.92 and 2.45 mg OC m^{-2} in the uncultivated grassland, respectively.

3.3. Iron oxide contribution to the specific mineral surface area ($SSA_{Feoxide}$)

Cultivated soils had lower $SSA_{Feoxide}$ in the upper 40 cm in both eroding and depositional positions, compared with the uncultivated grassland (Fig. 4). The $\%SSA_{Feoxide}$ tended to be lower in eroding (22 ± 7.7%) than in depositional (37 ± 5.8%) positions in uncultivated topsoils (~20 cm depth) while these percentages were smaller in the cultivated soils (9.5% eroding versus 5.9% depositional).

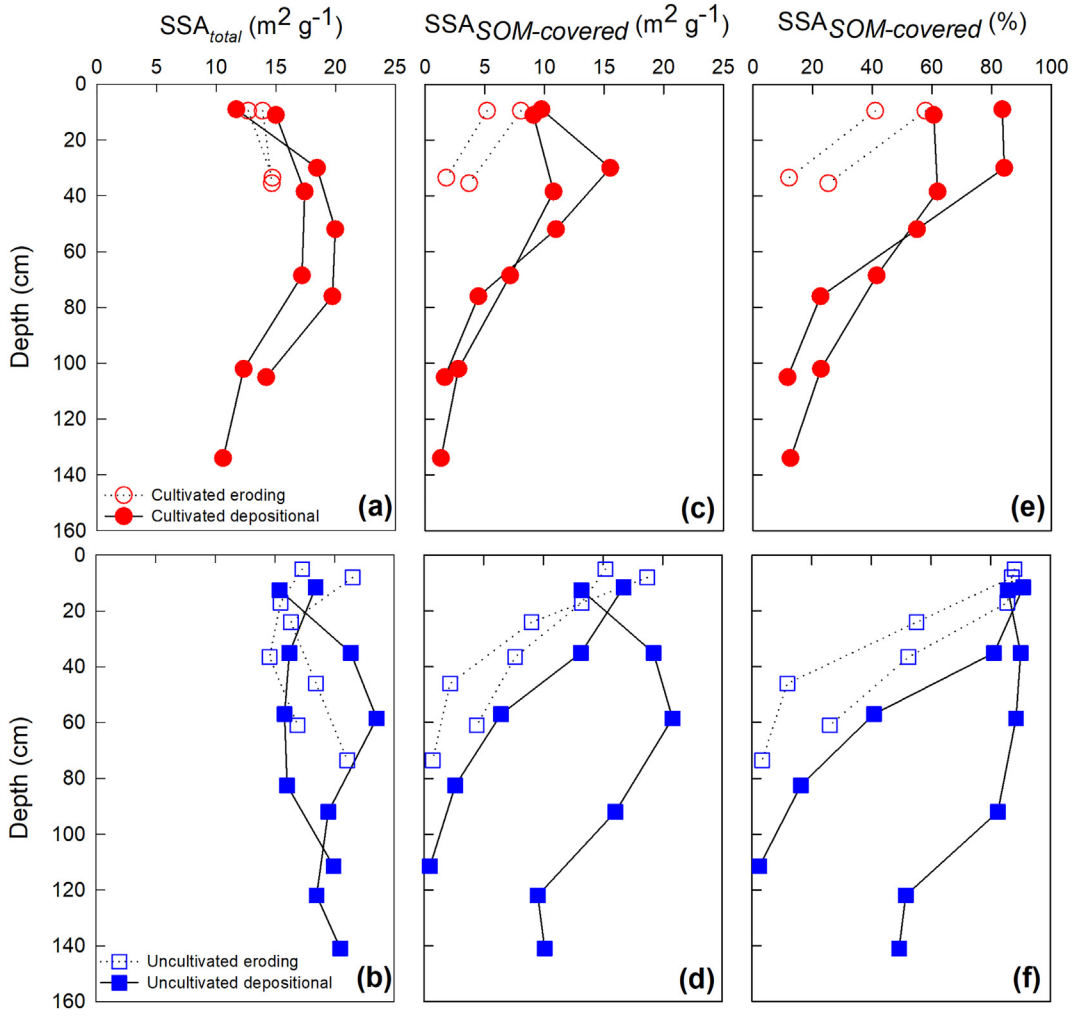

Fig. 2. Summary of SSA_{total}, $SSA_{SOM\text{-}covered}$, and $\%SSA_{SOM\text{-}covered}$ in the eroding and depositional sites of cultivated (agriculture) and uncultivated (grassland) hillslopes. (a, b) Total specific mineral surface area (SSA_{total}; m^2 g^{-1}). (c, d) The surface area covered by SOM ($SSA_{SOM\text{-}covered}$ m^2 g^{-1}). The percentage of total SSA covered by SOM ($\%SSA_{SOM\text{-}covered}$).

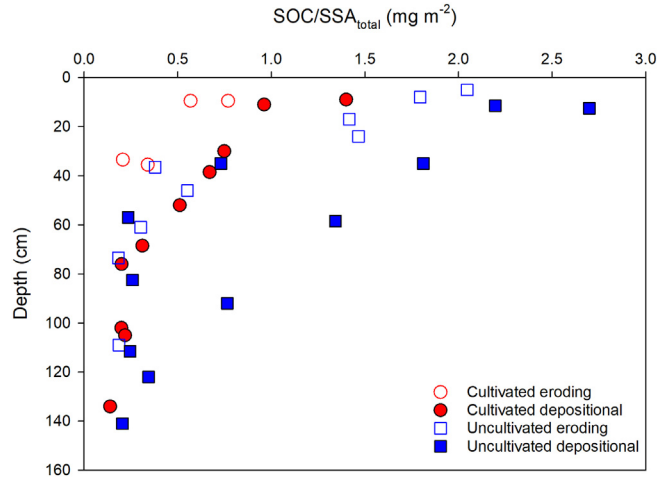

Fig. 3. Depth distribution of soil organic carbon loading (SOC/SSA$_{total}$ ratios) in the cultivated (agriculture) and uncultivated (grassland) eroding and depositional positions of hillslopes.

3.4. Extractable Fe oxides and clay content

Concentrations of extractable Fe oxides did not appear to differ by land use (6.9 ± 1.0 mg g^{-1} cultivated vs. 6.9 ± 0.9 mg g^{-1} uncultivated in eroding topsoils; and 5.8 ± 0.1 mg g^{-1} cultivated vs. 6.1 ± 0.0 mg g^{-1} uncultivated in depositional topsoils). Clay contents were also similar in the cultivated and uncultivated soils for eroding (25.8 ± 0.8 and 22.5 ± 4.5%, respectively) and depositional (19.8 ± 2.2 and 17.5 ± 0.5%, respectively) positions (Fig. 5c and d). Clay contents were relatively higher in eroding positions than in depositional positions at both hillslopes.

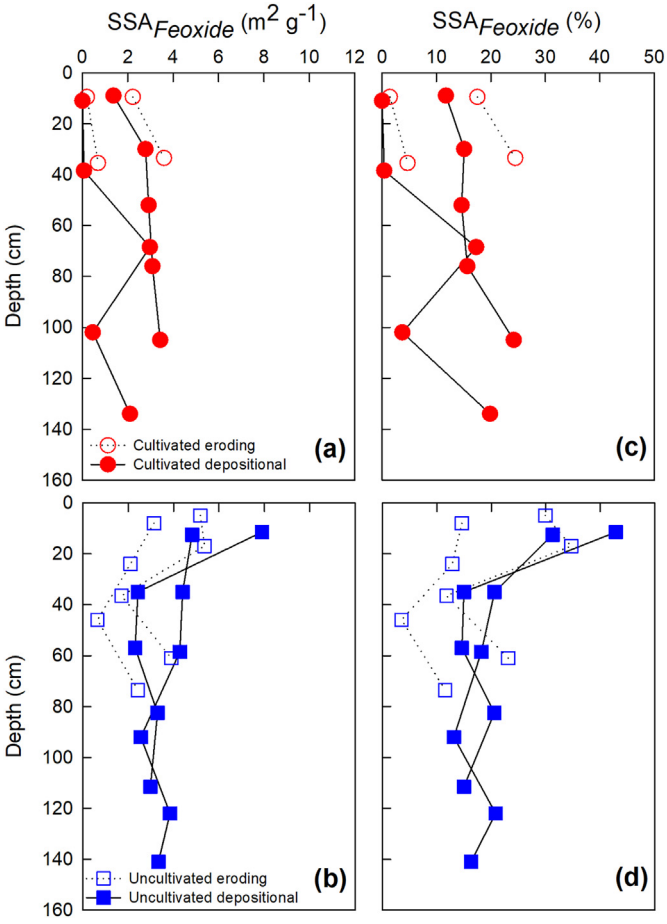

Fig. 4. Iron oxides contribution to SSA$_{total}$ (SSA$_{Feoxide}$; m^2 g^{-1}) (a and b) and percentage of SSA$_{total}$ contributed by Fe oxides (SSA$_{Feoxide}$) (c and d) from eroding and depositional positions of cultivated (agriculture) and uncultivated (grassland) hillslopes.

3.5. Chemical composition of soil organic matter associated with minerals

The chemical speciation of mineral-associated SOM in eroding soils clearly differed between the cultivated and uncultivated sites (Fig. 6 a and c). In cultivated eroding soils, the intensities of aromatic (284.8 eV) and phenolic (286.4 eV) C peaks were substantially weaker than in uncultivated grassland (Fig. 6). In the two depositional soils, the C speciation of mineral-associated SOM was similar between the cultivated and uncultivated hillslopes and was dominated by aromatic (284.8 eV), phenolic (286.4 eV), aliphatic (287.2 eV) C, amide and carboxyl (288.4 eV) C functional groups (Fig. 6). Although inorganic carbonate signals (290.1 eV) were detected in all soil samples, the signal is substantially subdued in the topsoil of the uncultivated grassland hillslope (Fig. 6). In contrast, the inorganic carbonate signals are pronounced in the topsoils of cultivated hillslope regardless of topographic position (Fig. 6).

The speciation of C in mineral-associated SOM differed substantially between eroding and depositional soils in both cultivated and uncultivated sites (Fig. 6). This was particularly true for subsoil samples where clear peaks associated with phenolic (286.4 eV) and aliphatic C (287.2 eV) were present in depositional positions, while these peaks were weak or absent in soil samples from eroding positions (Fig. 6). Furthermore, in the cultivated topsoil samples, aromatic (284.8 eV) and phenolic C (286.4 eV) peaks were more intense at depositional points than eroding points, while this difference was not found for the topsoil samples at the uncultivated site.

Similar to C speciation, N speciation changed with depth in the uncultivated eroding soil, and this is shown particularly in the decrease of heterocyclic-N peak intensity (398.8 eV) with depth (Fig. 7). The N speciation for the two eroding subsoils is the same within the signal: noise and the change in N speciation with depth for the cultivated site (eroding and depositional) are weak. The speciation of N-containing SOM associated with minerals was similar in depositional positions from cultivated and uncultivated hillslopes.

4. Discussion

4.1. Soil organic matter coverage of mineral surfaces

Long-term soil cultivation was associated with decreased SSA$_{SOM\text{-}covered}$ and %SSA$_{SOM\text{-}covered}$, regardless of landscape position (Fig. 2). Soil cultivation often results in breaking macro-aggregates which may enhance the decomposition of SOM (Ewing et al., 2006; Six et al., 2002). Reduced SOC concentrations and storage may also occur in agricultural systems due to annual biomass harvest (Papiernik et al., 2005). In addition, intensive cultivation physically disrupts soil structure and soil temperature regimes, accelerating SOM decomposition (Solomon et al., 2007). Therefore, it is likely that reduced SOM availability for physical/chemical interactions with soil minerals may have contributed to the decrease in SSA$_{SOM\text{-}covered}$ in the cultivated soils relative to the uncultivated grassland soils in the present study. Alternatively, the lower SSA$_{Feoxide}$ in the cultivated hillslopes (Fig. 4) could result in a lower potential for the SOM-mineral association and subsequent physical protection in the cultivated samples (Kleber et al., 2015; Mikutta et al., 2006). Regardless of the relative importance of these two explanations, the data indicates that tillage, which mixes SOM and minerals and thus has the potential to facilitate their physical contact (Yoo et al., 2011), may not lead to greater coverage of minerals by SOM. Similar observations related to the effects of soil mixing have been made for forested

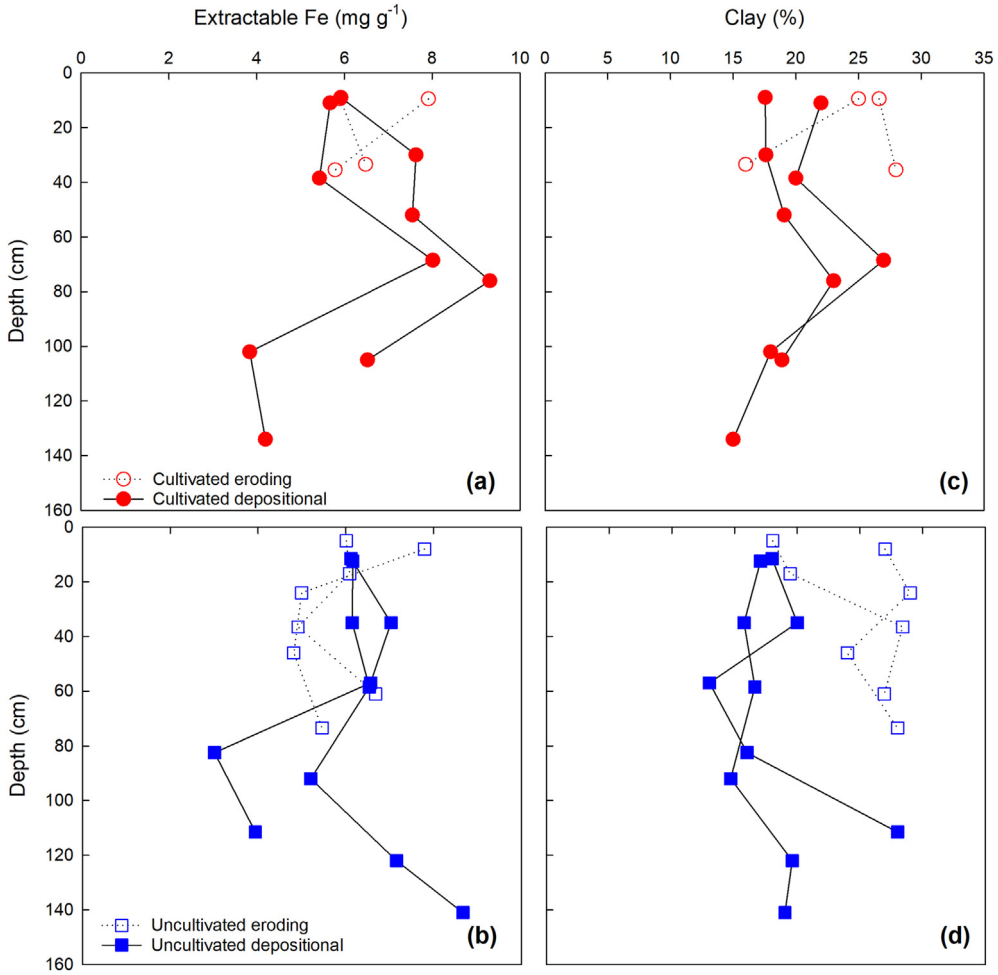

Fig. 5. Concentrations of extractable Fe oxides (mg g^{-1}) (a and b) extracted by the dithionite-citrate-bicarbonate method and clay (%) (c and d) in soil profiles form the eroding and depositional positions of cultivated (agriculture) and uncultivated (grassland) hillslopes, respectively.

systems in Minnesota where SOM loading to minerals is originally limited by the SSA_{total} prior to bioturbation by invasive earthworms but later by the SOM availability post earthworm invasion (Lyttle et al., 2015). These observations suggest that soil mixing may not be a limiting factor in the coverage of the mineral surface by organic matter in agricultural soils.

$SSA_{SOM\text{-}covered}$ in soils increased from eroding to depositional positions in both cultivated and uncultivated sites, but this increase is substantially larger in the cultivated hillslope (Fig. 2). These differences are associated with a simultaneous reduction in the exposed SSA_{total} and a corresponding increase in $SSA_{SOM\text{-}covered}$. Considering that the SSA_{total} does not differ significantly between eroding and depositional positions at both sites (Fig. 2), preferential transport of particular mineral groups or sizes (Fig. 5) appears not to be responsible for the observed topographic differences in $SSA_{SOM\text{-}covered}$. Instead, the higher $SSA_{SOM\text{-}covered}$ in depositional settings (Fig. 3) may be due to the greater availability of SOM in those landscape positions (Table 1). Studies have shown that SOM in different size classes can be preferentially transported from upslope eroding to the downslope depositional positions (Berhe et al., 2012; Lal, 2003; Wang et al., 2014). Greater vegetative biomass has been frequently observed in depositional areas in both cultivated and uncultivated systems, providing more plant carbon input into soils at these locations (Papiernik et al., 2005; Yoo et al., 2006). Thus, at depositional locations, the combined pool of SOM eroded from the upslope areas and greater in-situ plant carbon input in the low-lying positions may have provided a larger pool of SOM available for mineral association.

Processes that are responsible for greater SOM coverage of mineral surfaces in the low-lying hillslope positions appears to be more effective at the cultivated site. Minerals in eroding soils on the cultivated site are coated with SOM by less than ~60% (Fig. 2), and some fractions of the remaining SSA may scavenge additional SOM during sediment transport and/or post-deposition. Alternatively, accelerated erosion in the cultivated site has exposed subsoil minerals with lower proportional coverage by SOM, and topsoils had been redistributed to the depositional slope. In contrast to the cultivated hillslope, topsoils in the eroding portion of the uncultivated grassland hillslope show that nearly 90% of the total SSA is covered with SOM, and this percentage does not increase at all in the depositional soils (Fig. 2). The remaining 10% of the total SSA may originate from primary minerals with little capacity to scavenge SOM. This indicates that an additional amount of SOM newly scavenged by minerals during the sediment movement within the hillslope is minimal in the uncultivated grassland hillslope.

Another potential process responsible for the greater SOM coverage of mineral surface in lower hillslope locations may involve the persistent burial of soils by new sediments in the depositional portion of hillslopes. In the steeper uncultivated hillslope, the extent that $SSA_{SOM\text{-}covered}$ decreases with increasing depth is substantially subdued at depositional locations relative to eroding locations. Exponential decreases in decomposition rates with increasing soil depth has been observed in numerous field and laboratory experiments (Doetterl et al., 2012; Pries et al., 2017; Wang et al., 2013) and thus have become a foundation for modeling the development of SOC depth profiles (Jobbágy and Jackson, 2000; Kramer et al., 2017; Lorenz and Lal,

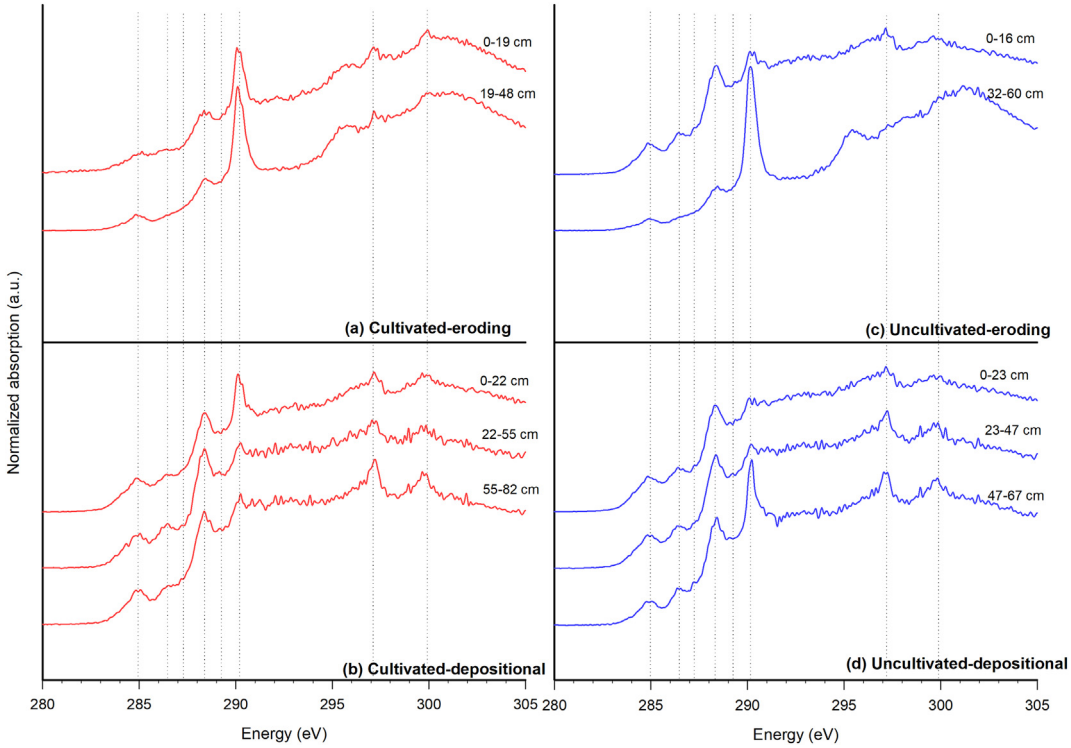

Fig. 6. X-ray absorption near edge fine structure (XANES) spectra at C 1 s edge for fine heavy fractions (<250 μm and >2.0 g cm^{-3}) as a function of soil depth from cultivated and uncultivated (grassland) soil. Vertical dashed lines indicate resonances of (1) aromatic, (2) phenolic, (3) aliphatic, (4) amide and carboxyl C, (5) O-alkyl and (6) carbonyl and carbonate. The peaks at 297 and 300 eV results indicate the L_3 and L_2 edges of potassium.

2005). The combination of such depth-dependent decomposition and rapid burial of the depositional soils by a continuous supply of sediments from upslope may have contributed to the greater SOM coverage of mineral surface in lower hillslope locations (Fig. 2). This process is also active in the cultivated hillslope as shown by little to no depth-dependency of $SSA_{SOM\text{-}covered}$ in depositional soils (Fig. 2).

Our results showed that the depositional sites had higher SOC loading (mg OC m^{-2}) than the eroding sites at the two hillslopes (Fig. 3). A

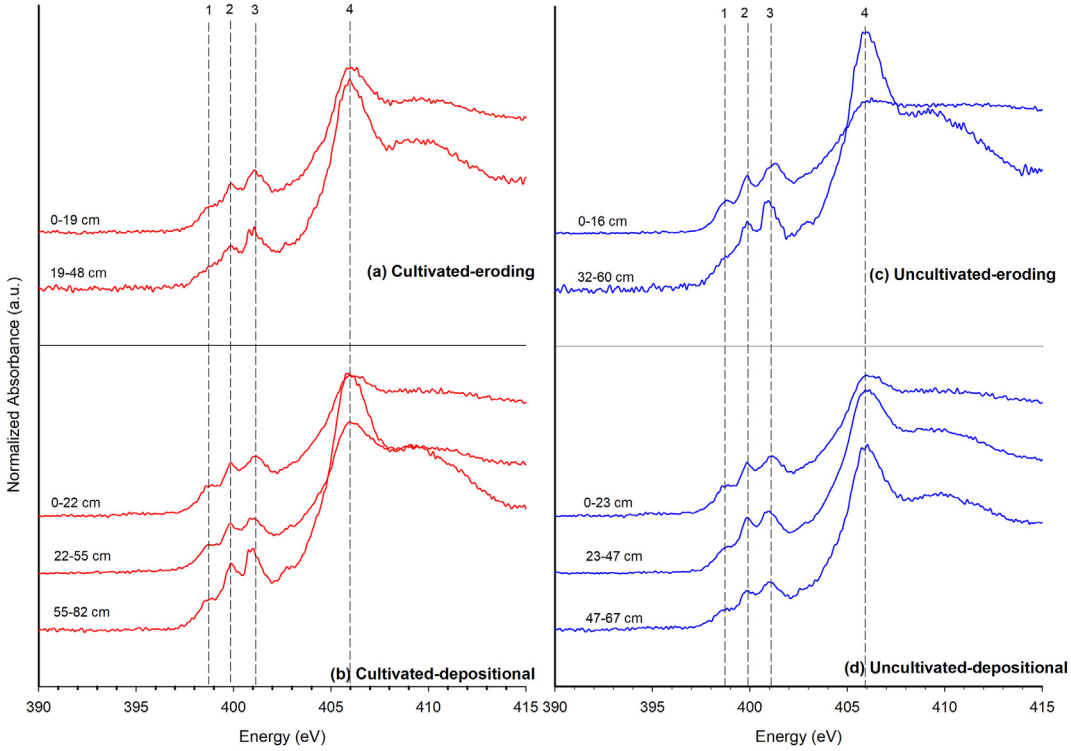

Fig. 7. Nitrogen (N) 1 s edge XANES for fine heavy fractions (<250 μm and >2.0 g cm^{-3}) as a function of depth from cultivated and uncultivated eroding and depositional positions. Nitrogen features are assigned as (1) aromatic-N in 6-membered rings at 398.8 eV (heterocyclic-N); (2) nitrilic and aromatic N in 5-membered rings at 399.9 eV (pyrazolic); (3) amide with possible contributions from pyrroles at 401.3 eV (amide); and (4) alkyl-N, inorganic NH_4^+, and the 1 s → σ* feature at 406.0 eV (alkyl-N).

similar study conducted for a forested hillslope underlain by metamorphosed sedimentary rocks in southeastern Pennsylvania (Fisher et al., 2018) found that soil creep and mixing via tree root growth and tree falls had promoted the formation of mineral-associated SOM such that SOC loadings and inventories were larger by a factor of 2–3 in the depositional soils than in the upslope eroding soils. The similar trend that depositional sites have larger SOC loading on the mineral surface the eroding sites was observed in grassland, cropland (Fig. 3) and forested transects (Fisher et al., 2018). This comparison allows us to suggest that the scavenging of new SOM by eroded minerals is an integral part of sediment redistribution process and is common in a wide range of vegetation types, sediment transport processes, and agricultural management schemes.

4.2. The contribution of Fe oxides to the total mineral surface area ($SSA_{Feoxide}$, $\%SSA_{Feoxide}$)

In our study, Fe oxides provided up to 43% of the SSA_{total} among all of the studied samples (Fig. 4), confirming that oxides have the potential to be an important source of surface area across a diverse range of soil types (Eusterhues et al., 2005; Pronk et al., 2011; Wissing et al., 2014).

In the cultivated soils, mineral surface area attributed to Fe oxides ($SSA_{Feoxide}$) and its relative contribution to the total mineral surface area ($\%SSA_{Feoxide}$) is smaller than in the uncultivated soils, and this difference is most pronounced in the topsoils (Fig. 4). Contrarily, we observed similar extractable Fe concentrations in topsoils regardless of land use (Fig. 5). $SSA_{Feoxide}$ is thus not directly controlled by the abundance of extractable Fe oxides in soils. Long-term agricultural management may thus have involved significant changes in the types of extractable Fe oxides present (Pronk et al., 2011; Wissing et al., 2014). It is also possible that B horizons materials, which are now exposed by accelerated erosion, may include different types of Fe oxides. For instance, ferrihydrite minerals have SSA values of 200–400 $m^2\ g^{-1}$, and fresh "hydrous Fe oxides" have SSA values of 305–412 $m^2\ g^{-1}$, while crystalline Fe oxides have SSA of 116–184 $m^2\ g^{-1}$ (Borggaard, 1982; Cornell and Schwertmann, 2003). Although extractable Fe oxides, quantified using the dithionite-citrate extraction method, had been previously found in greater quantities in depositional positions compared with the eroding positions (Berhe et al., 2012; Ellerbrock et al., 2016; Wang et al., 2013), such topographic trends were not present at our studied hillslopes. Nonetheless, the observed decoupling between $SSA_{Feoxides}$ and extractable Fe oxide concentrations warns against equating greater Fe oxide pools with a greater surface area capable of interacting with SOM.

4.3. Chemical speciation of carbon and nitrogen in mineral-associated soil organic matter

In the topsoil for all landscape positions, the C speciation of mineral-associated SOM featured three major peaks representing aromatic, phenolic, amide/carboxylic, and carbonate moieties (Fig. 6). These C species have been commonly observed for SOM in organo-mineral assemblages, clay-size fractions, and micro-aggregates (Chen and Sparks, 2015; Kleber et al., 2011; Solomon et al., 2005). The presence of phenols indicates the presence of the plant-derived C from lignin degradation in the mineral-associated SOM pool (Goñi and Hedges, 1992; Solomon et al., 2009, 2005). In eroding soils at both hillslopes, interactions of decomposed plant-derived compounds and minerals (as indicated by the intensity of phenolic peaks) appear to be limited to shallow depths among the samples analyzed. The phenolic C was largely limited to the topsoils in at eroding locations (Fig. 6). In contrast, soils at depositional locations (regardless of land use) showed the persistence of phenolic C throughout all analyzed sample depths. This indicates that burial of SOM by sediments may contribute to preserving phenolic compounds (Chen and Sparks, 2015). Furthermore, aromatic and amide/carboxylic C, which is likely derived from microbial proteins and other biomolecules in bacterial cells (Gillespie et al., 2011; Keiluweit et al., 2012; Solomon et al., 2009, 2005), was found across all samples analyzed in this study. These observations indicate that SOM derived from microbial turnover is not only an important component of the mineral-associated SOM pool (Rumpel et al., 2015) but is ubiquitous in mineral-associated SOM pools regardless of land use, topography, and depth.

The prominence of amide N mineral-associated SOM (Fig. 7) across all samples is consistent with the previous observations that proteinaceous N is the dominant form of organic N in soils at all depths (Schnitzer et al., 2006; Schulten and Schnitzer, 1997).

The speciation of C in the mineral-associated SOM pool in eroding topsoil differed between the cultivated and uncultivated grassland hillslopes (Fig. 6), with the main difference being a much weaker phenolic C signal in the cultivated-eroding topsoil. This depletion of phenolic C could be explained by increased decomposition or low inputs of the plant-derived C due to the agricultural removal of plant materials (Goñi and Hedges, 1992; Rumpel et al., 2009; Solomon et al., 2007). This agrees with our earlier interpretation of lower $SSA_{SOM\text{-}covered}$ observed in the cultivated eroding soils. Such biological depletion of phenolic C inputs must have outweighed the effects of tillage practices, which vertically mix soils (Yoo et al., 2011), resulting in the absence of phenolic signals in the subsoil as well (Fig. 6).

In depositional positions, the speciation of C and N in mineral-associated SOM appeared to be similar across the sample locations, regardless of land use (Fig. 6). These C and N speciation data, when examined in the context of the mineral surface area presented above, provide new insight into the nature of SOM that is newly scavenged by minerals during the transport and deposition of eroded sediments. In the cultivated eroding hillslope, minerals in the topsoil are only half covered by SOM, and mineral-associated SOM in the soils has lower levels of phenolic C. In depositional soils, however, 60–80% of the total mineral surface area was covered by SOM, and mineral-associated SOM exhibits phenolic C, as well as aromatic, amide, and carboxyl C-associated peaks. The similar speciation of C and N in mineral-associated SOM in the depositional positions in both cultivated and uncultivated hillslopes (Figs. 6 and 7) may indicate newly scavenged SOM obtained during sediment redistribution within the cultivated site does not appear to differ chemically from the mineral-associated SOM in the uncultivated depositional soils.

5. Conclusion

The combined use of X-ray absorption spectroscopy and specific mineral surface area determination is a novel approach to characterizing the formation of mineral-associated SOM during hillslope sediment redistribution and its sensitivity to agricultural management. Long-term cultivation and erosion decreased the $SSA_{SOM\text{-}covered}$ in both eroding (by 61% in topsoil) and depositional (by 37% in topsoil) positions, respectively. Depositional positions had a relatively larger $SSA_{SOM\text{-}covered}$ compared with the upper eroding positions. Furthermore, our data indicate that long-term cultivation affects the speciation of C in mineral-associated SOM by decreasing aromatic C and enhancing the degradation of plant-derived lignin in eroding soils. However, our data also suggest that eroded soils may recapture a fraction of this C through interactions with minerals during hillslope sediment transport.

Acknowledgment

Carbon and nitrogen spectroscopy reported in this paper was performed at the Canadian Light Source (CLS), which is supported by the Canada Foundation for Innovation, Natural Sciences and Engineering Research Council of Canada, the University of Saskatchewan, the Government of Saskatchewan, Western Economic Diversification Canada, the National Research Council Canada, and the Canadian Institutes of Health Research. We also thank J. Dynes, T. Regier, and Z. Arthur for their

assistance at the CLS's SGM beamline. This work was funded by a National Science Foundation grant to Yoo (EAR1253198) and in part by a National Science Foundation Graduate Research Fellowship to N.A. Jelinski. The authors wish to acknowledge and express sincere gratitude to a large body of visionary work conducted at the study site regarding the landscape-scale quantification of erosion rates and the effects of land use and erosion on crop yields and soil properties by S.K. Papiernik, D.A. Lobb, T.E. Schumacher, M.J. Lindstrom, A. Farenhorst, S. DeAlba, D.D. Malo, K.D. Stephens, J.A. Schumacher, M.L. Lieser, A. Eynard, and S. Li.

References

Amundson, R., Berhe, A.A., Hopmans, J.W., Olson, C., Sztein, A.E., Sparks, D.L., 2015. Soil and human security in the 21st century. Science 348, 1261071. https://doi.org/10.1126/science.1261071.

Berhe, A.A., Harden, J.W., Torn, M.S., Kleber, M., Burton, S.D., Harte, J., 2012. Persistence of soil organic matter in eroding versus depositional landform positions. J. Geophys. Res. Biogeosci. 117, G02019. https://doi.org/10.1029/2011JG001790.

Besnard, E., Chenu, C., Balesdent, J., Puget, P., Arrouays, D., 1996. Fate of particulate organic matter in soil aggregates during cultivation. Eur. J. Soil Sci. 47, 495–503. https://doi.org/10.1111/j.1365-2389.1996.tb01849.x.

Borggaard, O.K., 1982. The influence of iron oxides on the surface area of soil. J. Soil Sci. 33, 443–449. https://doi.org/10.1111/j.1365-2389.1982.tb01779.x.

Brandes, J.A., Lee, C., Wakeham, S., Peterson, M., Jacobsen, C., Wirick, S., Cody, G., 2004. Examining marine particulate organic matter at sub-micron scales using scanning transmission X-ray microscopy and carbon X-ray absorption near edge structure spectroscopy. Mar. Chem. 92, 107–121. https://doi.org/10.1016/j.marchem.2004.06.020.

Brunauer, S., Emmett, P.H., Teller, E., 1938. Adsorption of gases in multimolecular layers. J. Am. Chem. Soc. 60, 309–319. https://doi.org/10.1021/ja01269a023.

Chen, C., Sparks, D.L., 2015. Multi-elemental scanning transmission X-ray microscopy–near edge X-ray absorption fine structure spectroscopy assessment of organo–mineral associations in soils from reduced environments. Environ. Chem. 12, 64–73. https://doi.org/10.1071/EN14042.

Cornell, R.M., Schwertmann, U., 2003. The Iron Oxides: Structure, Properties, Reactions, Occurrences and Uses. John Wiley & Sons.

Cusack, D.F., Chadwick, O.A., Ladefoged, T., Vitousek, P.M., 2013. Long-term effects of agriculture on soil carbon pools and carbon chemistry along a Hawaiian environmental gradient. Biogeochemistry 112, 229–243. https://doi.org/10.1007/s10533-012-9718-z.

De Alba, S., Lindstrom, M., Schumacher, T.E., Malo, D.D., 2004. Soil landscape evolution due to soil redistribution by tillage: a new conceptual model of soil catena evolution in agricultural landscapes. Catena 58, 77–100. https://doi.org/10.1016/j.catena.2003.12.004.

Dignac, M.-F., Derrien, D., Barré, P., Barot, S., Cécillon, L., Chenu, C., Chevallier, T., Freschet, G.T., Garnier, P., Guenet, B., Hedde, M., Klumpp, K., Lashermes, G., Maron, P.-A., Nunan, N., Roumet, C., Basile-Doelsch, I., 2017. Increasing soil carbon storage: mechanisms, effects of agricultural practices and proxies. A review. Agron. Sustain. Dev. 37, 14. https://doi.org/10.1007/s13593-017-0421-2.

Doetterl, S., Six, J., Van Wesemael, B., Van Oost, K., 2012. Carbon cycling in eroding landscapes: geomorphic controls on soil organic C pool composition and C stabilization. Glob. Chang. Biol. 18, 2218–2232. https://doi.org/10.1111/j.1365-2486.2012.02680.x.

Don, A., Schumacher, J., Freibauer, A., 2011. Impact of tropical land-use change on soil organic carbon stocks – a meta-analysis. Glob. Chang. Biol. 17, 1658–1670. https://doi.org/10.1111/j.1365-2486.2010.02336.x.

Ellerbrock, R.H., Gerke, H.H., Deumlich, D., 2016. Soil organic matter composition along a slope in an erosion-affected arable landscape in north east Germany. Soil Tillage Res. 156, 209–218. https://doi.org/10.1016/j.still.2015.08.014.

Eusterhues, K., Rumpel, C., Kögel-Knabner, I., 2005. Organo-mineral associations in sandy acid forest soils: importance of specific surface area, iron oxides and micropores. Eur. J. Soil Sci. 56, 753–763. https://doi.org/10.1111/j.1365-2389.2005.00710.x.

Ewing, S.A., Sanderman, J., Baisden, W.T., Wang, Y., Amundson, R., 2006. Role of large-scale soil structure in organic carbon turnover: evidence from California grassland soils. J. Geophys. Res. Biogeosci. 111, G03012. https://doi.org/10.1029/2006JG000174.

Fisher, B.A., Aufdenkampe, A.K., Yoo, K., Aalto, R.E., Marquard, J., 2018. Soil carbon redistribution and organo-mineral associations after lateral soil movement and mixing in a first-order forest watershed. Geoderma 319, 142–155. https://doi.org/10.1016/j.geoderma.2018.01.006.

Gillespie, A.W., Walley, F.L., Farrell, R.E., Regier, T.Z., Blyth, R.I.R., 2008. Calibration method at the N K-edge using interstitial nitrogen gas in solid-state nitrogen-containing inorganic compounds. J. Synchrotron Radiat. 15, 532–534. https://doi.org/10.1107/S0909049508014283.

Gillespie, A.W., Walley, F.L., Farrell, R.E., Leinweber, P., Eckhardt, K.-U., Regier, T.Z., Blyth, R.I.R., 2011. XANES and pyrolysis-FIMS evidence of organic matter composition in a hummocky landscape. Soil Sci. Soc. Am. J. 75, 1741–1755. https://doi.org/10.2136/sssaj2010.0279.

Gillespie, A.W., Phillips, C.L., Dynes, J.J., Chevrier, D., Regier, T.Z., Peak, D., 2015. Advances in using soft X-Ray spectroscopy for measurement of soil biogeochemical processes. Advances in Agronomy. Elsevier, pp. 1–32 https://doi.org/10.1016/bs.agron.2015.05.003.

Goñi, M.A., Hedges, J.I., 1992. Lignin dimers: structures, distribution, and potential geochemical applications. Geochim. Cosmochim. Acta 56, 4025–4043. https://doi.org/10.1016/0016-7037(92)90014-A.

Guggenberger, G., Zech, W., Haumaier, L., Christensen, B.t., 1995. Land-use effects on the composition of organic matter in particle-size separates of soils: II. CPMAS and solution ^{13}C NMR analysis. Eur. J. Soil Sci. 46, 147–158. https://doi.org/10.1111/j.1365-2389.1995.tb01821.x.

Harris, K., 2003. Geologic atlas of Pope County. Minn. Minn. Geol. Surv. Cty.

Heister, K., 2014. The measurement of the specific surface area of soils by gas and polar liquid adsorption methods—limitations and potentials. Geoderma 216, 75–87. https://doi.org/10.1016/j.geoderma.2013.10.015.

Helfrich, M., Ludwig, B., Buurman, P., Flessa, H., 2006. Effect of land use on the composition of soil organic matter in density and aggregate fractions as revealed by solid-state ^{13}C NMR spectroscopy. Geoderma 136, 331–341. https://doi.org/10.1016/j.geoderma.2006.03.048.

IUSS Working Group WRB, 2014. World Reference Base for Soil Resources 2014 International Soil Classification System for Naming Soils and Creating Legends for Soil Maps. FAO, Rome.

Jackson, R.B., Lajtha, K., Crow, S.E., Hugelius, G., Kramer, M.G., Piñeiro, G., 2017. The ecology of soil carbon: pools, vulnerabilities, and biotic and abiotic controls. Annu. Rev. Ecol. Evol. Syst. 48, 419–445. https://doi.org/10.1146/annurev-ecolsys-112414-054234.

Jelinski, N.A., 2014. Problems of Physical Movement in Soil Genesis: Application of Meteoric Beryllium-10 as a Component of Multi-tracer Analysis. Ph.D. Thesis. University of Minnesota, United States — Minnesota.

Jobbágy, E.G., Jackson, R.B., 2000. The vertical distribution of soil organic carbon and its relation to climate and vegetation. Ecol. Appl. 10, 423–436. https://doi.org/10.1890/1051-0761(2000)010[0423:TVDOSO]2.0.CO;2.

Jokic, A., Cutler, J.N., Anderson, D.W., Walley, F.L., 2004. Detection of heterocyclic N compounds in whole soils using N-XANES spectroscopy. Can. J. Soil Sci. 84, 291–293. https://doi.org/10.4141/S03-094.

Kaiser, K., Guggenberger, G., 2003. Mineral surfaces and soil organic matter. Eur. J. Soil Sci. 54, 219–236. https://doi.org/10.1046/j.1365-2389.2003.00544.x.

Keiluweit, M., Bougoure, J.J., Zeglin, L.H., Myrold, D.D., Weber, P.K., Pett-Ridge, J., Kleber, M., Nico, P.S., 2012. Nano-scale investigation of the association of microbial nitrogen residues with iron (hydr)oxides in a forest soil O-horizon. Geochim. Cosmochim. Acta 95, 213–226. https://doi.org/10.1016/j.gca.2012.07.001.

Kleber, M., Nico, P.S., Plante, A., Filley, T., Kramer, M., Swanston, C., Sollins, P., 2011. Old and stable soil organic matter is not necessarily chemically recalcitrant: implications for modeling concepts and temperature sensitivity. Glob. Chang. Biol. 17, 1097–1107. https://doi.org/10.1111/j.1365-2486.2010.02278.x.

Kleber, M., Eusterhues, K., Keiluweit, M., Mikutta, C., Mikutta, R., Nico, P.S., 2015. Mineral–organic associations: formation, properties, and relevance in soil environments. Advances in Agronomy. Elsevier, pp. 1–140 https://doi.org/10.1016/bs.agron.2014.10.005.

Kögel-Knabner, I., Guggenberger, G., Kleber, M., Kandeler, E., Kalbitz, K., Scheu, S., Eusterhues, K., Leinweber, P., 2008. Organo-mineral associations in temperate soils: integrating biology, mineralogy, and organic matter chemistry. J. Plant Nutr. Soil Sci. 171, 61–82. https://doi.org/10.1002/jpln.200700048.

Konert, M., Vandenberghe, J., 1997. Comparison of laser grain size analysis with pipette and sieve analysis: a solution for the underestimation of the clay fraction. Sedimentology 44, 523–535. https://doi.org/10.1046/j.1365-3091.1997.d01-38.x.

Kramer, M.G., Lajtha, K., Audfenkampe, A., 2017. Depth trends of soil organic matter C:N and ^{15}N natural abundance controlled by association with minerals. Biogeochemistry, 1–12 https://doi.org/10.1007/s10533-017-0378-x.

Lal, R., 2003. Soil erosion and the global carbon budget. Environ. Int. 29, 437–450. https://doi.org/10.1016/S0160-4120(02)00192-7.

Leinweber, P., Kruse, J., Walley, F.L., Gillespie, A., Eckhardt, K.-U., Blyth, R.I.R., Regier, T., 2007. Nitrogen K-edge XANES – an overview of reference compounds used to identify `unknown' organic nitrogen in environmental samples. J. Synchrotron Radiat. 14, 500–511. https://doi.org/10.1107/S0909049507042513.

Li, S., Lobb, D.A., Lindstrom, M.J., Farenhorst, A., 2007. Tillage and water erosion on different landscapes in the northern north American Great Plains evaluated using ^{137}Cs technique and soil erosion models. Catena 70, 493–505. https://doi.org/10.1016/j.catena.2006.12.003.

Li, S., Lobb, D.A., Lindstrom, M.J., Papiernik, S.K., Farenhorst, A., 2008. Modeling tillage-induced redistribution of soil mass and its constituents within different landscapes. Soil Sci. Soc. Am. J. 72, 167–179. https://doi.org/10.2136/sssaj2006.0418.

Lorenz, K., Lal, R., 2005. The depth distribution of soil organic carbon in relation to land use and management and the potential of carbon sequestration in subsoil horizons. Advances in Agronomy. Academic Press, pp. 35–66 https://doi.org/10.1016/S0065-2113(05)88002-2.

Lyttle, A., Yoo, K., Hale, C., Aufdenkampe, A., Sebestyen, S.D., Resner, K., Blum, A., 2015. Impact of exotic earthworms on organic carbon sorption on mineral surfaces and soil carbon inventories in a northern hardwood forest. Ecosystems 18, 16–29. https://doi.org/10.1007/s10021-014-9809-x.

Martens, D.A., Reedy, T.E., Lewis, D.T., 2004. Soil organic carbon content and composition of 130-year crop, pasture and forest land-use managements. Glob. Chang. Biol. 10, 65–78. https://doi.org/10.1046/j.1529-8817.2003.00722.x.

Mayer, L.M., Xing, B., 2001. Organic matter–surface area relationships in acid soils. Soil Sci. Soc. Am. J. 65, 250–258. https://doi.org/10.2136/sssaj2001.651250x.

Mehra, O.P., Jackson, M.L., 2013. Iron oxide removal from soils and clays by a dithionite–citrate system buffered with sodium bicarbonate. In: Ingerson, E. (Ed.), Clays and Clay Minerals. Pergamon, pp. 317–327 https://doi.org/10.1016/B978-0-08-009235-5.50026-7.

Mikutta, R., Kaiser, K., 2011. Organic matter bound to mineral surfaces: resistance to chemical and biological oxidation. Soil Biol. Biochem. 43, 1738–1741. https://doi.org/10.1016/j.soilbio.2011.04.012.

Mikutta, R., Kleber, M., Torn, M.S., Jahn, R., 2006. Stabilization of soil organic matter: association with minerals or chemical recalcitrance? Biogeochemistry 77, 25–56. https://doi.org/10.1007/s10533-005-0712-6.

Mikutta, R., Mikutta, C., Kalbitz, K., Scheel, T., Kaiser, K., Jahn, R., 2007. Biodegradation of forest floor organic matter bound to minerals via different binding mechanisms. Geochim. Cosmochim. Acta 71 (10), 2569–2590. https://doi.org/10.1016/j.gca.2007.03.002.

Miller, B.A., Schaetzl, R.J., 2012. Precision of soil sample particle size results using laser diffractometry. Soil Sci. Soc. Am. J. 76 (5), 1719–1727. https://doi.org/10.2136/sssaj2011.0303.

Minnesota County Biological Survey, 2003. Native Plant Communities and Rare Species in Pope County, Minnesota. State of Minnesota Department of Natural Resources http://files.dnr.state.mn.us/eco/mcbs/maps/pope.pdf.

Papiernik, S.K., Lindstrom, M.J., Schumacher, J.A., Farenhorst, A., Stephens, K.D., Schumacher, T.E., Lobb, D.A., 2005. Variation in soil properties and crop yield across an eroded prairie landscape. J. Soil Water Conserv. 60, 388–395.

Papiernik, S.K., Lindstrom, M.J., Schumacher, T.E., Schumacher, J.A., Malo, D.D., Lobb, D.A., 2007. Characterization of soil profiles in a landscape affected by long-term tillage. Soil Tillage Res. 93, 335–345. https://doi.org/10.1016/j.still.2006.05.007.

Papiernik, S.K., Schumacher, T.E., Lobb, D.A., Lindstrom, M.J., Lieser, M.L., Eynard, A., Schumacher, J.A., 2009a. Soil properties and productivity as affected by topsoil movement within an eroded landform. Soil Tillage Res. 102, 67–77. https://doi.org/10.1016/j.still.2008.07.018.

Papiernik, S.K., Koskinen, W.C., Yates, S.R., 2009b. Solute transport in eroded and rehabilitated prairie landforms. 2. Reactive solute. J. Agric. Food Chem. 57, 7434–7439. https://doi.org/10.1021/jf901334t.

Pisani, O., Haddix, M.L., Conant, R.T., Paul, E.A., Simpson, M.J., 2016. Molecular composition of soil organic matter with land-use change along a bi-continental mean annual temperature gradient. Sci. Total Environ. 573, 470–480. https://doi.org/10.1016/j.scitotenv.2016.08.154.

Pries, C.E.H., Castanha, C., Porras, R.C., Torn, M.S., 2017. The whole-soil carbon flux in response to warming. Science 355, 1420–1423. https://doi.org/10.1126/science.aal1319.

Prokop, P., Kruczkowska, B., Syiemlieh, H.J., Bucala-Hrabia, A., 2018. Impact of topography and sedentary swidden cultivation on soils in the hilly uplands of north-east India. Land Degrad. Dev., 1–11 https://doi.org/10.1002/ldr.3018.

Pronk, G.J., Heister, K., Kögel-Knabner, I., 2011. Iron oxides as major available interface component in loamy arable topsoils. Soil Sci. Soc. Am. J. 75, 2158–2168. https://doi.org/10.2136/sssaj2010.0455.

Ravel, B., Newville, M., 2005. ATHENA, ARTEMIS, HEPHAESTUS: data analysis for X-ray absorption spectroscopy using IFEFFIT. J. Synchrotron Radiat. 12, 537–541. https://doi.org/10.1107/S0909049505012719.

Regier, T., Krochak, J., Sham, T., Hu, Y., Thompson, J., Blyth, R., 2007. Performance and capabilities of the Canadian dragon: the SGM beamline at the Canadian Light Source. Nucl. Instrum. Methods Phys. Res., Sect. A 582, 93–95. https://doi.org/10.1016/j.nima.2007.08.071.

Rumpel, C., Ba, A., Darboux, F., Chaplot, V., Planchon, O., 2009. Erosion budget and process selectivity of black carbon at meter scale. Geoderma 154, 131–137. https://doi.org/10.1016/j.geoderma.2009.10.006.

Rumpel, C., Baumann, K., Remusat, L., Dignac, M.-F., Barré, P., Deldicque, D., Glasser, G., Lieberwirth, I., Chabbi, A., 2015. Nanoscale evidence of contrasted processes for root-derived organic matter stabilization by mineral interactions depending on soil depth. Soil Biol. Biochem. 85, 82–88. https://doi.org/10.1016/j.soilbio.2015.02.017.

Sanderman, J., Hengl, T., Fiske, G.J., 2017. Soil carbon debt of 12,000 years of human land use. Proc. Natl. Acad. Sci. 114, 9575–9580. https://doi.org/10.1073/pnas.1706103114.

Schnitzer, M., McArthur, D.F.E., Schulten, H.-R., Kozak, L.M., Huang, P.M., 2006. Long-term cultivation effects on the quantity and quality of organic matter in selected Canadian prairie soils. Geoderma 130, 141–156. https://doi.org/10.1016/j.geoderma.2005.01.021.

Schulten, H.-R., Schnitzer, M., 1997. The chemistry of soil organic nitrogen: a review. Biol. Fertil. Soils 26, 1–15. https://doi.org/10.1007/s003740050335.

Six, J., Conant, R.T., Paul, E.A., Paustian, K., 2002. Stabilization mechanisms of soil organic matter: implications for C-saturation of soils. Plant Soil 241, 155–176. https://doi.org/10.1023/A:1016125726789.

Kellogg soil survey laboratory methods manual. In: Soil Survey Staff, Burt, R., Soil Survey Staff (Eds.), Soil SurveyInvestigations Report No. 42, Version 5.0. U.S. Department of Agriculture, Natural Resources Conservation Service.

Soil Survey Staff, 2014. Keys to soil taxonomy by soil survey staff. 12th ed. Soil Conservation Service 12. United States Department of Agriculture, Natural Resources Conservation Service, Washington, DC.

Sollins, P., Kramer, M.G., Swanston, C., Lajtha, K., Filley, T., Aufdenkampe, A.K., Wagai, R., Bowden, R.D., 2009. Sequential density fractionation across soils of contrasting mineralogy: evidence for both microbial- and mineral-controlled soil organic matter stabilization. Biogeochemistry 96, 209–231. https://doi.org/10.1007/s10533-009-9359-z.

Solomon, D., Lehmann, J., Kinyangi, J., Liang, B., Schäfer, T., 2005. Carbon K-edge NEXAFS and FTIR-ATR spectroscopic investigation of organic carbon speciation in soils. Soil Sci. Soc. Am. J. 69, 107–119. https://doi.org/10.2136/sssaj2005.0107dup.

Solomon, D., Lehmann, J., Kinyangi, J., Amelung, W., Lobe, I., Pell, A., Riha, S., Ngoze, S., Verchot, L., Mbugua, D., Skjemstad, J., Schäfer, T., 2007. Long-term impacts of anthropogenic perturbations on dynamics and speciation of organic carbon in tropical forest and subtropical grassland ecosystems. Glob. Chang. Biol. 13, 511–530. https://doi.org/10.1111/j.1365-2486.2006.01304.x.

Solomon, D., Lehmann, J., Kinyangi, J., Liang, B., Heymann, K., Dathe, L., Hanley, K., Wirick, S., Jacobsen, C., 2009. Carbon (1s) NEXAFS spectroscopy of biogeochemically relevant reference organic compounds. Soil Sci. Soc. Am. J. 73, 1817–1830. https://doi.org/10.2136/sssaj2008.0228.

University of Minnesota, John R. Borchert Map Library, 2017. Minnesota Historical Aerial Photographs Online. https://www.lib.umn.edu/apps/mhapo/, Accessed date: 20 December 2017.

Van Oost, K., Quine, T.A., Govers, G., De Gryze, S., Six, J., Harden, J.W., Ritchie, J.C., McCarty, G.W., Heckrath, G., Kosmas, C., Giraldez, J.V., 2007. The impact of agricultural soil erosion on the global carbon cycle. Science 318, 626–629. https://doi.org/10.1126/science.1145724.

Van Oost, K., Verstraeten, G., Doetterl, S., Notebaert, B., Wiaux, F., Broothaerts, N., Six, J., 2012. Legacy of human-induced C erosion and burial on soil – atmosphere C exchange. Proc. Natl. Acad. Sci. 109, 19492–19497. https://doi.org/10.1073/pnas.1211162109.

Wagai, R., Mayer, L.M., Kitayama, K., 2009. Extent and nature of organic coverage of soil mineral surfaces assessed by a gas sorption approach. Geoderma 149, 152–160. https://doi.org/10.1016/j.geoderma.2008.11.032.

Wang, X., Cammeraat, L.H., Wang, Z., Zhou, J., Govers, G., Kalbitz, K., 2013. Stability of organic matter in soils of the Belgian Loess Belt upon erosion and deposition. Eur. J. Soil Sci. 64, 219–228. https://doi.org/10.1111/ejss.12018.

Wang, X., Cammeraat, E.L.H., Cerli, C., Kalbitz, K., 2014. Soil aggregation and the stabilization of organic carbon as affected by erosion and deposition. Soil Biol. Biochem. 72, 55–65. https://doi.org/10.1016/j.soilbio.2014.01.018.

Wang, X., Yoo, K., Mudd, S.M., Weinman, B., Gutknecht, J., Gabet, E.J., 2018. Storage and export of soil carbon and mineral surface area along an erosional gradient in the Sierra Nevada, California. Geoderma 321, 151–163. https://doi.org/10.1016/j.geoderma.2018.02.008.

Wissing, L., Kölbl, A., Schad, P., Bräuer, T., Cao, Z.-H., Kögel-Knabner, I., 2014. Organic carbon accumulation on soil mineral surfaces in paddy soils derived from tidal wetlands. Geoderma 228–229, 90–103. https://doi.org/10.1016/j.geoderma.2013.12.012.

Yoo, K., Amundson, R., Heimsath, A.M., Dietrich, W.E., 2006. Spatial patterns of soil organic carbon on hillslopes: integrating geomorphic processes and the biological C cycle. Geoderma 130, 47–65. https://doi.org/10.1016/j.geoderma.2005.01.008.

Yoo, K., Ji, J., Aufdenkampe, A., Klaminder, J., 2011. Rates of soil mixing and associated carbon fluxes in a forest versus tilled agricultural field: implications for modeling the soil carbon cycle. J. Geophys. Res. Biogeosci. 116, G01014. https://doi.org/10.1029/2010JG001304.

Zhu, H., Wu, J., Guo, S., Huang, D., Zhu, Q., Ge, T., Lei, T., 2014. Land use and topographic position control soil organic C and N accumulation in eroded hilly watershed of the Loess Plateau. Catena 120, 64–72. https://doi.org/10.1016/j.catena.2014.04.007.